Sensitivity analysis for the design optimisation of an energy tunnel based hydronic heated pavement

Transportation Geotechnics 58 (2026) 101921

Contents lists available at ScienceDirect

Transportation Geotechnics

journal homepage: www.elsevier.com/locate/trgeo

Original Article

A comparative assessment of the bearing capacity of unselected construction and demolition waste aggregates in unbound and cement-stabilised pavement subbases

Luca Tefa, Marco Bassani *

Department of Environment, Land and Infrastructure Engineering, Politecnico di Torino, Torino, Italy

A R T I C L E I N F O

Keywords:
Cement-stabilised materials
Construction and demolition waste
Road subbase
Lightweight deflectometer
Plate loading test

A B S T R A C T

Using unselected construction and demolition waste (UCDW) aggregate helps the road construction industry to meet sustainability requirements. Although the use of recycled UCDW aggregates is increasingly recognised and adopted in practice, there remains limited field evidence directly comparing their performance with that of natural (NAT) aggregates in unbound and cement-stabilised subbases. This study compared the bearing capacity of four 30-cm subbases (unbound and 3% cement-stabilised NAT and UCDW) using lightweight deflectometer and plate loading tests on an experimental road. The study was complemented by laboratory resilient modulus and indirect tensile strength measurements on specimens compacted during the construction activities.

On average, the surface modulus of unbound UCDW materials was 16% higher than that of natural aggregates. Stabilisation with 3% cement significantly increased the bearing capacity sevenfold for UCDW materials and tenfold for NAT materials. After three days of curing, the average surface modulus increased from 112.3–126.6 MPa for unbound UCDW and 95.2–111.6 MPa for unbound NAT, to 884.7–1024.6 MPa for cement-stabilised UCDW and 1064.3–1198.1 MPa for cement-stabilised NAT. Unlike the field tests, where cement-stabilised NAT performed slightly better than cement-stabilised UCDW, the laboratory tests showed that cement-stabilised UCDW mixtures had a higher resilient modulus than cement-stabilised natural ones. These results demonstrate that UCDW aggregates can effectively replace natural ones in the formation of unbound or cement–stabilised road subbase layers.

Introduction

In industrialised countries, the ageing road network requires a constant supply of materials for maintenance purposes [1,2]. Despite the emergence of new circular economy policies that advocate for the use of recycled materials in road construction, professionals, contractors and road agencies are reluctant to adopt these policies due to concerns regarding consistency with technical specifications, field performance and environmental regulations [3,4].

It is estimated that more than one-third of the total waste generated in Europe in 2022 (860 million tonnes) came from construction and demolition activities, making this waste stream the main source of waste for recycled aggregate production [5].

Construction and demolition waste (CDW) aggregates are generally classified into two categories [6,7]. “Selected” aggregates derive from selective demolition processes [8] and allow for relatively high reuse rates in new concrete (15–30%) and asphalt mixtures (up to 50%) [9,10]. However, the production of these materials is currently subject

Abbreviations: AASHTO, American Association of State Highway and Transportation Officials; ANOVA, Analysis of Variance; ASTM, American Standard for Testing Materials; CDW, Construction and Demolition Waste; CNR, *Centro Nazionale delle Ricerche* (Italian); COV, Coefficient of Variation; CS, Cement-Stabilised; CS-NAT, Cement-Stabilised Natural Aggregate mixture; CS-UCDW, Cement-Stabilised Unselected Construction and Demolition Waste Aggregate mixture; DD_{situ}, In-situ Dry Density; E_{LWD}, Surface Modulus derived from LWD measurements; EN, European Standard; M-EPDG, Mechanistic-Empirical Pavement Design Guide; H, High (stress level); ITS, Indirect Tensile Strength; L, Low (stress level); LWD, Lightweight Deflectometer; M, Medium (stress level); MC_{situ}, In-situ Moisture Content; MDD, Maximum Dry Density; M_{PLT}, Strain modulus from the 1st loading cycle of the plate loading test; M'_{PLT}, Strain modulus from the 2nd loading cycle of the plate loading test; NAT, Natural Aggregate; OMC, Optimum Moisture Content; PLT, Plate Loading Test; RH, Relative Humidity; RM, Resilient Modulus; SD, Standard Deviation; SE, Standard Error; SEE, Standard Error of the Estimate; SEM, Standard Error of the Mean; UCDW, Unselected Construction and Demolition Waste.

* Corresponding author.
E-mail addresses: luca.tefa@polito.it (L. Tefa), marco.bassani@polito.it (M. Bassani).

https://doi.org/10.1016/j.trgeo.2026.101921
Received 11 September 2025; Received in revised form 7 January 2026; Accepted 24 January 2026
Available online 26 January 2026

to time-consuming and costly separation processes. In contrast, "unselected" CDW (UCDW) aggregates are derived from mixed, unsorted demolition debris, but their heterogeneous composition, which depends on the materials used, limits their suitability for structural applications [11]. Nevertheless, owing to their economic benefits and adequate performance in applications involving low loads [12], UCDW aggregates are increasingly used in foundations, embankments and lower pavement layers [13]. Evidence suggests that UCDW aggregates could conveniently be used in the unbound and stabilised subbases of road pavements [6,14–16], where traffic-induced stresses are comparatively low due to the shielding effect of the upper layers [17]. In unbound granular subbases, the mechanical bearing capacity is mainly provided by aggregate interlock, gradation, and compaction [18,19]. While recycled aggregates from UCDW can offer comparable stiffness when well compacted [20], their behaviour may differ from NAT aggregates because of higher water absorption, heterogeneous composition, and a greater tendency for particle breakage during compaction and loading [6,21]. For cement-stabilised subbases, the formation of a bonded skeleton through hydration products significantly enhances stiffness and strength [22]. However, the effectiveness of stabilisation can vary depending on the quality of the aggregates (e.g., NAT vs. UCDW materials), moisture distribution, and curing [23,24]. The promotion of UCDW aggregates for use in road construction is often hindered by concerns that their promising laboratory performance may not be replicated on a large scale. While the majority of studies have investigated the field properties of "selected" CDW materials [25–28], very few have evaluated the performance of UCDW aggregate. Tavira et al. [29] reported lower back-calculated moduli for UCDW subbases compared with natural aggregates, recommending an increased thickness that could offset the environmental benefits of UCDW material. Similarly, Beja et al. [30] monitored the bearing capacity of different subbase layers made with (i) unbound, (ii) cement-stabilised, and (iii) lime-treated UCDW aggregates over a period of 18 months. Improved performance was observed when UCDW was treated with cement or lime. However, the absence of a direct comparison with natural aggregates prevented the true structural implications of substitution from being assessed.

To the best of our knowledge, previous studies have not comprehensively compared NAT and UCDW aggregates in unbound and cement-stabilised subbases under the same conditions in a full–scale test. This study addresses this gap by comparing the bearing capacity of subbases made with UCDW and natural (NAT) aggregate in both unbound and cement-stabilised (CS) states through a controlled, full-scale experimental design in which all materials were produced, placed, compacted and tested simultaneously and under identical environmental and structural conditions.

A 140 m long experimental road was constructed (Fig. 1), incorporating four different 30 cm-thick subbases containing unbound NAT, unbound UCDW, CS-NAT and CS-UCDW (with 3% in weight of cement). Complementary laboratory tests were also performed to classify and characterise the materials, enabling the field results to be robustly interpreted and meaningfully compared with the findings of previous studies. The experimental design was intentionally limited to a controlled comparison between NAT and UCDW, and although the full-scale road constrained the number of variables that could be tested, statistical robustness was ensured through extensive replication and formal statistical analyses.

Materials and methods

Experimental plan

Four subbase materials were compared in this study. Two of these materials were unbound, while the other two were cement-stabilised. The aggregates used in their production were NAT and UCDW. The bearing capacity of a pavement layer is conventionally assessed by measuring its deflection under a reference load, with the extent of deflection depending on the material's stiffness [31].

In this study, the bearing capacity was measured using a lightweight deflectometer (LWD), while the stiffness of the constituent materials was determined by measuring their resilient modulus using repeated load triaxial tests on samples prepared with the same mixtures as those used on-site. As the objective was to compare material performance under identical structural conditions, a formal pavement structural design was not performed. The thickness of all subbases was set at 30 cm with each subbase placed on a 40 cm-thick subgrade made of unbound UCDW aggregate (Fig. 2), in accordance with standard Italian practice for local roads [32,33].

With this configuration, we assumed that the pressure bulb generated by the LWD plate would remain largely confined within the subbase, thereby limiting the supporting layer's contribution to the

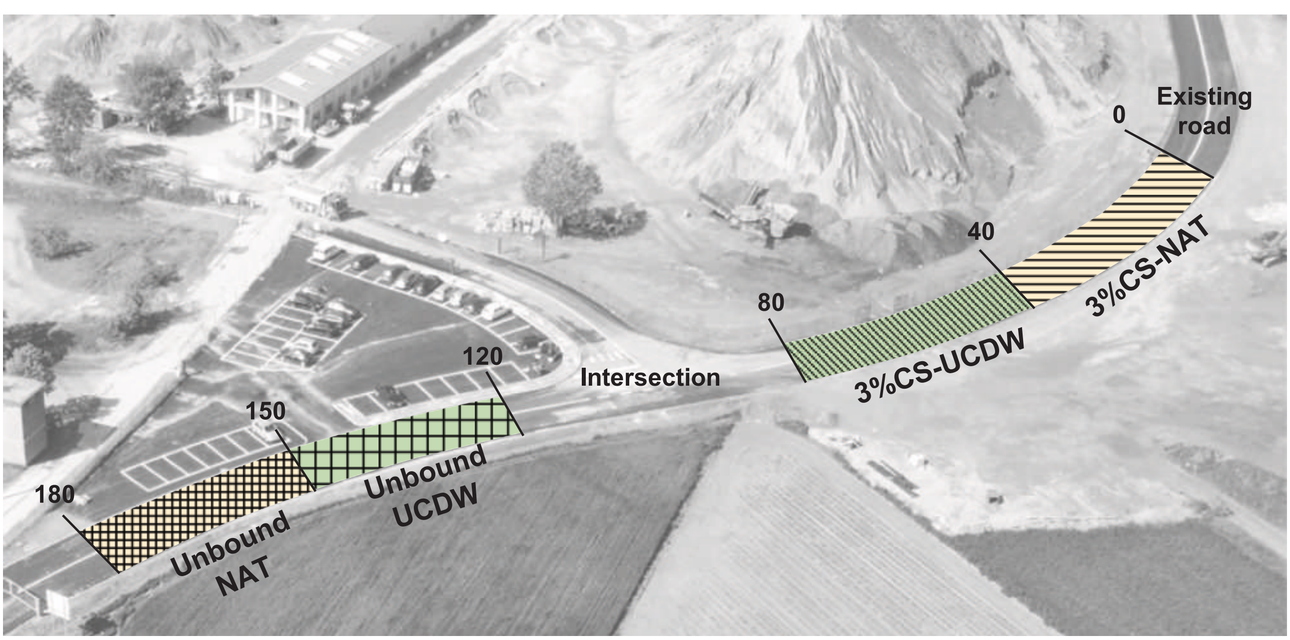

Fig. 1. Aerial picture of the experimental road with the four testing sections.

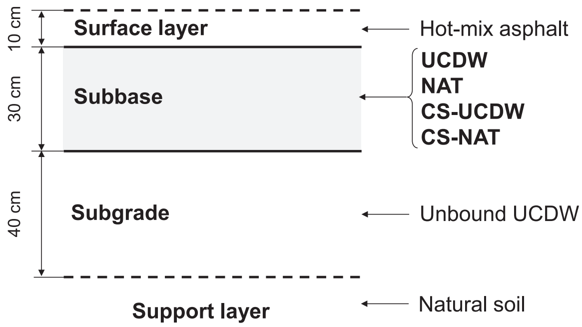

Fig. 2. Pavement structure of the experimental road.

subbase's response. A 10-cm-thick surface layer of hot-mix asphalt was laid after the completion of the testing programme on the subbase.

Materials

Aggregates

The UCDW aggregate was provided by *Cavit S.p.A.*, a construction company based in La Loggia, Italy. Its recycling facility processes waste from demolition, reclamation and excavation activities, producing an average of 250,000 Mg of UCDW per year through cleaning, crushing and screening operations. A 0–40 mm size fraction was employed in the construction of the subgrade and subbase layers of the experimental road. The particle size distribution as per EN 933-1 [34] (Fig. 3), the shape index, the flakiness index, the particle density, and the distribution of the main UCDW constituents (Table 1) were determined for four different samples collected during the construction phase of the experimental road. An analysis of the composition of the UCDW aggregate revealed a significant presence of concrete particles and natural aggregate (averaging 24.4% and 52.5%, respectively), together with more limited quantities of bricks and tiles, and bituminous materials. The variability in the composition of the UCDW aggregate is due to the variability in the waste stream collected and treated at the recycling facility [6].

The NAT aggregate, with a size fraction of 0–40 mm, was sourced from the *Cave Germaire* quarry (Carignano, Italy) and transported to the construction site in dump trucks. Two separate samples were collected during the experimental road construction for preliminary testing. The results of these tests are shown in Fig. 3 and Table 1. The gradation of the NAT aggregate closely aligns with that of the UCDW material, with both falling within the 0–45 mm range of granular material for subbase layers as indicated by the Italian Technical Specifications [32]. There is minimal disparity between the shape and flakiness indices for the NAT and UCDW materials. However, the particle density value for the NAT aggregate is significantly higher than that for the UCDW aggregate due to the presence of lighter constituent materials (e.g., bricks and impurities) in the latter. The two aggregates were intentionally selected to exhibit similar basic physical characteristics, thereby enabling a comparison that isolates the influence of their origin (natural versus recycled) from confounding effects related to particle size distribution and shape.

Table 1
Average and standard deviation (SD) of shape index, flakiness index, particle density, and constituent classification of UCDW and NAT aggregates (R_c = concrete, concrete products, mortar; R_u = unbound aggregate, natural stone; R_b = bricks and tiles, R_a = bituminous materials, X = impurities like metals, wood, plastic, rubber, etc.).

Parameter		UCDW	NAT	Reference standard
Shape index (%)		13.0 ± 1.4	13.5 ± 0.7	EN 933-4 [35]
Flakiness index (%)		12.0 ± 1.6	12.5 ± 0.7	EN 933-3 [36]
Particle density (Mg/m^3)		2.445 ± 0.035	2.630 ± 0.028	EN 1097-6 [37]
Composition (%)	Concrete (R_c)	24.4 ± 8.1	–	EN 933-11 [38]
	Unbound aggregate (R_u)	52.5 ± 8.1	100	
	Bricks and tiles (R_b)	13.3 ± 0.4	–	
	Bituminous materials (R_a)	9.3 ± 4.1	–	
	Impurities (X)	0.7 ± 0.2	–	

Mix-design and production of subbase mixtures

Prior to the construction of the experimental road, a modified Proctor compaction test was performed in accordance with EN 13286-2 [35] to determine the optimum moisture content (OMC) and the maximum dry density (MDD) for each mixture [36]. Fig. 4 shows the same OMCs for both stabilised and unbound mixtures (8.5% for UCDW and 6.5% for NAT), despite the addition of 3% cement. The low cement

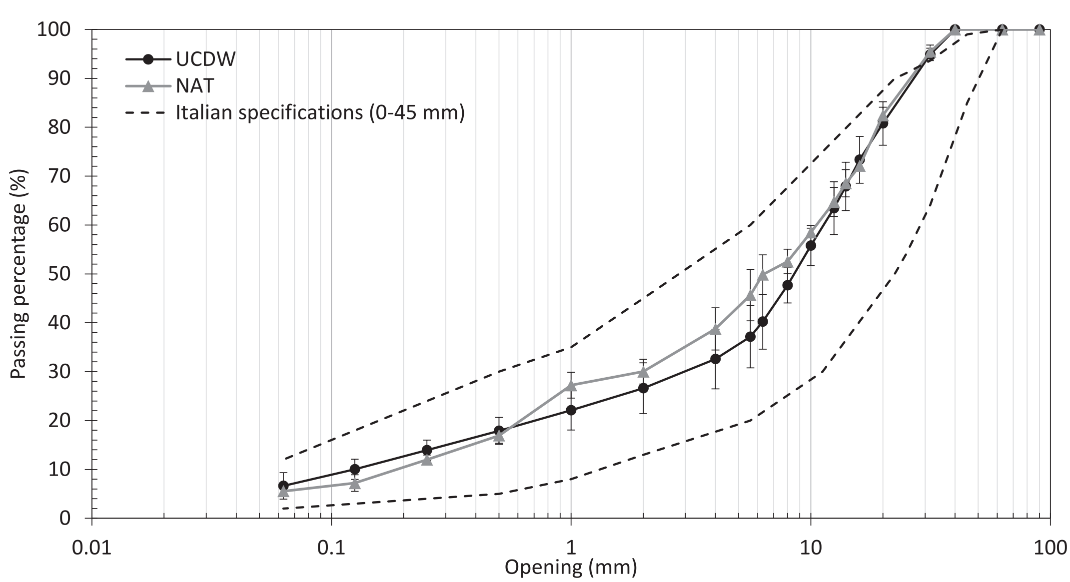

Fig. 3. Particle size distribution of (a) UCDW and (b) NAT aggregates. Error bars indicate one standard deviation (SD).

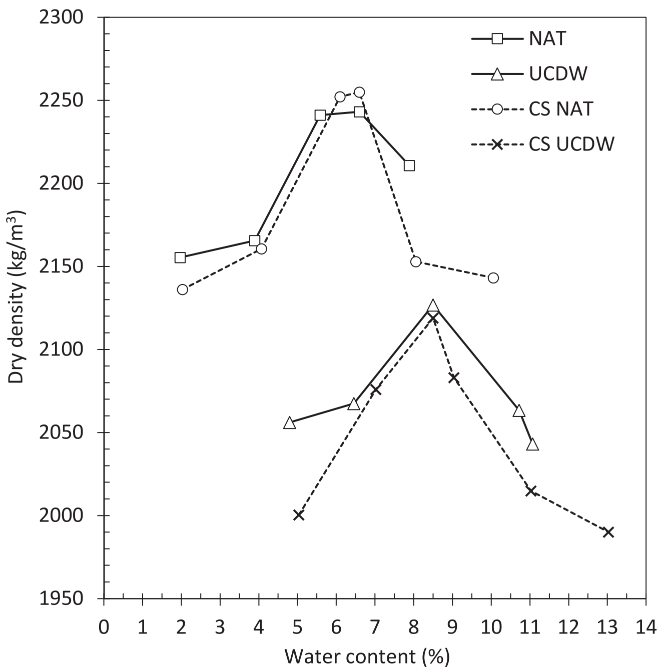

Fig. 4. Proctor compaction test results.

content did not measurably affect the compaction moisture demand in this specific study [23,37].

Table 2 lists the compaction parameters (OMC and MDD), the mix design, and the mixture designation of the subbase materials. The CS mixtures were produced in a mixing plant located 200 m from the construction site. CS mixtures were produced by adding 3% of cement to the dry mass of aggregates, in line with previous studies [38–40]. The Portland limestone cement used in this study was classified as CEM II/B-LL 32.5 R in accordance with EN 197-1 [41]. This cement type is composed of 65–79% clinker, 21–35% limestone, and 0–5% other constituents. This composition has been demonstrated to reduce the embodied CO_2 compared to traditional CEM-I, making it a more sustainable option. CEM II/B-LL is a popular choice for structural and geotechnical applications, and it is readily available in the local market due to the high availability of limestone in the region.

Testing methods and interpretation of results

The experimental investigation was organised as shown in Fig. 5.

Field tests

The bearing capacity of subgrade and subbase layers was measured through deflection tests with a *Dynatest 3032* LWD [27], in accordance with ASTM E2583-07 [42]. This equipment has an integrated plate loading cell with a range of 0–25.0 kN, an accuracy of 2% ± 2 kPa, and a precision 0.0003 kN, as well as a central geophone with a range of 0–2200 μm, an accuracy 2% ± 2 μm and a precision of 0.1 μm, for recording load and displacement time histories, respectively. To meet the sensitivity and accuracy of measurement requirements [43], the

Table 2
Mix-design and mixture designation with indication of Proctor compaction parameters.

Aggregate	Cement content	Mixture designation	OMC (%)	MDD (kg/m³)
UCDW	–	UCDW	8.5	2127
UCDW	3	CS-UCDW	8.5	2119
NAT	–	NAT	6.5	2243
NAT	3	CS-NAT	6.5	2255

plate diameter was 300 mm for the unbound materials and 200 mm for CS mixtures. The falling mass was kept constant at 20 kg, and the dropping height was set to 33, 58, and 84 cm to generate different stress levels and evaluate the stress-dependent behaviour of the materials [44,45]. Details of the stress levels are provided in Table 3. For each testing point, the LWD plate was centred and levelled prior to each drop. During the test, at least nine consecutive drops were applied. The first three drops were discarded as seating drops, and only stable measurements were retained for modulus calculation. Boussinesq's elastic theory was adopted to determine the surface modulus (E_{LWD}) assuming a stress distribution factor of 2 and Poisson's ratios of 0.35 and 0.25 for unbound and CS mixtures, respectively [46].

A static plate loading test (PLT) was conducted in accordance with the ASTM D1195 standard and adapted to meet the requirements of the Italian standard CNR 146/1992 [47]. A double-cycle static PLT was carried out using a 300 mm diameter plate, a 200 kN hydraulic jack, and three dial gauges (range 0–50,000 μm; resolution 1 μm; precision 6 μm; measuring force ≤2.1 N), which were positioned at 120° on the plate to c reaction frame (e.g., 20 tonne roller) was used to ensure uniform load transfer.

In the first cycle, the pressure was increased from 0.05 to 0.35 MPa in increments of 0.10 MPa. After an unloading step, a second loading cycle was applied in 0.10 MPa increments from 0.05 to 0.25 MPa. During each loading increment, the pressure was increased to the target value, after which it was held constant to allow the layer to undergo primary deformation. Settlement readings were then taken.

The strain moduli at the first loading cycle (M_{PLT}) and the second loading cycle (M'_{PLT}) were calculated using Eqs. (1) and (2), respectively, where Δp and $\Delta p'$ represent the pressure increments from 0.15 to 0.25 MPa for the first and second loading cycles, Δs and $\Delta s'$ represent the corresponding settlements for the first and second loading cycles, and D is the plate diameter (300 mm):

$$M_{PLT} = \frac{\Delta p}{\Delta s} \cdot D \quad (1)$$

$$M'_{PLT} = \frac{\Delta p'}{\Delta s'} \cdot D \quad (2)$$

The sand-cone test method, as defined in ASTM D1556-15 [48], was used to determine the dry density (DD_{situ}) of the subgrade and subbase materials in the field. A small hole was excavated at the test point, and the removed material was collected and weighed in the lab to determine the wet and dry masses and the water content. Next, a sand-cone apparatus filled with calibrated and uniformly graded sand was positioned over the hole and the volume of sand required to fill the cavity was measured. The in-situ dry density was then calculated using the dry mass of the material, the measured sand volume, and the water content of the sample.

Each of the four subbase sections was characterised by eight LWD drops, as well as two PLT and two in-situ density tests. All field tests were carried out three days after construction. Testing points were randomly selected on a 1 × 1 m grid, with the exclusion of the first and final 4 m of each section, and the outer 1 m of the two lateral edges. The PLT and sand-cone tests were conducted at points adjacent to those tested with the LWD. Figs. 6 and 7 show the locations of the testing points for the unbound and cement-stabilised subbases, respectively.

Laboratory tests

During the construction of the experimental road, the subbase materials were sampled to produce cylindrical specimens for laboratory testing (see Fig. 8c, d). Before compaction, both the unbound and CS mixtures were sieved to a maximum size of 25 mm to ensure the 100 mm diameter specimens did not contain any larger particles. This inevitably introduced differences in the gradation between the laboratory (0–25 mm) and the field material (0–40 mm). However, because this preparatory step was applied identically to all mixtures, any influence it

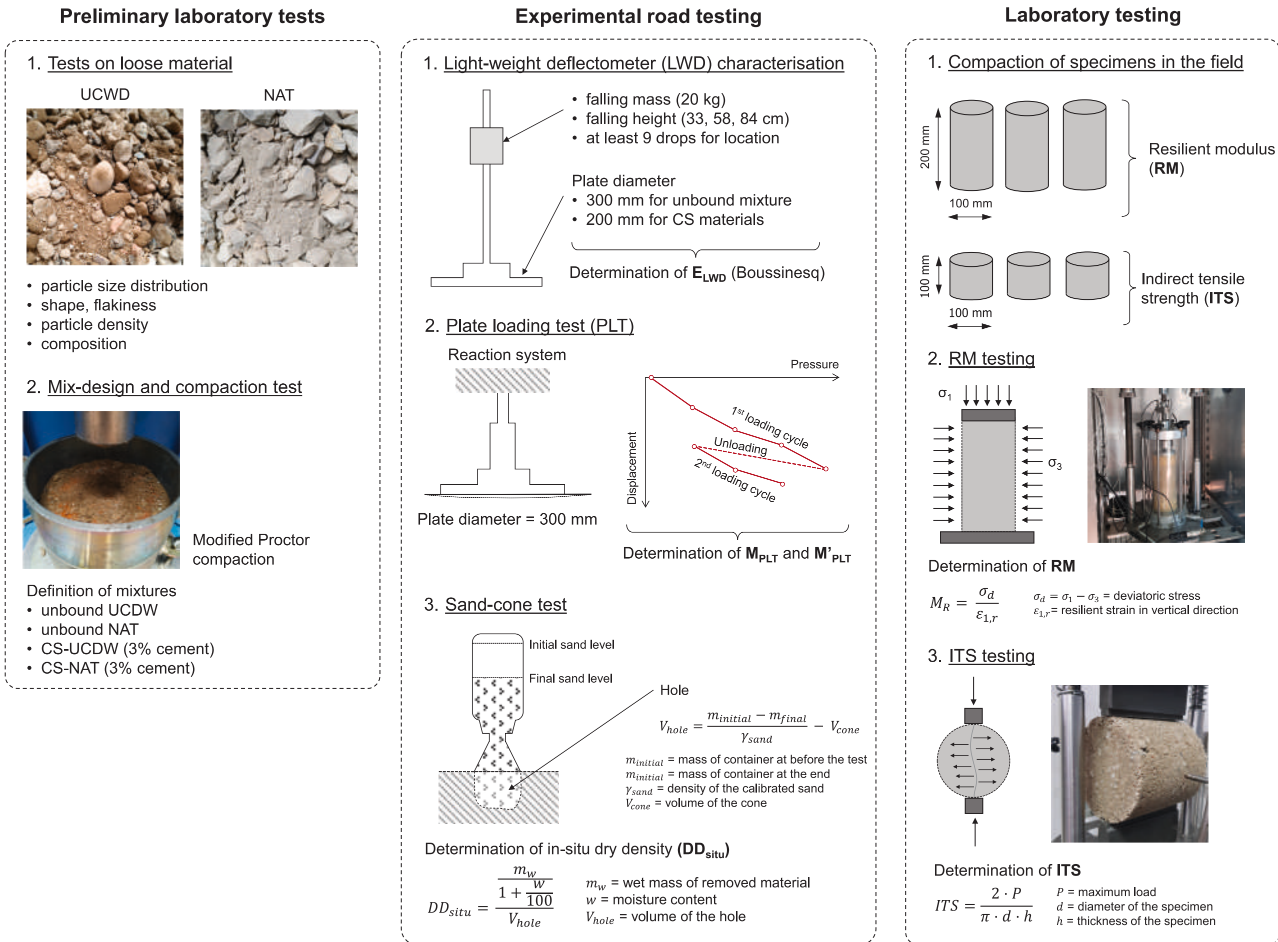

Fig. 5. Experimental plan.

Table 3
Pressure ranges (in kPa) on the LWD loading plate.

Plate diameter (mm)	Dropping height (cm)		
	33	58	84
300	97–101	149–153	194–198
200	220–225	339–345	440–450
Stress level	Low (L)	Medium (M)	High (H)

introduced affected both materials equally. As a result, it did not compromise the comparative trends on which this study is based.

Two different geometries were produced: slender (100 × 200 mm, diameter × height) for resilient modulus (RM) tests, and stubby (100 × 100 mm, diameter × height) for indirect tensile strength (ITS) tests. The slender and stubby specimens were compacted into eight and four layers, respectively, with 25 blows per layer administered to achieve the modified Proctor compaction energy of 2.6 MJ/m^3. After compaction, the samples were stored in split plastic moulds to prevent damage during transportation to the laboratory, then sealed in a plastic bag to prevent moisture loss. The unbound and CS mixtures were then cured in a temperature- and humidity-controlled room at 25 °C and a relative humidity (RH) above 90% for 7 and 28 days before testing. Three identical specimens were prepared for each material (i.e., unbound UCDW and NAT, and CS-UCDW and CS-NAT) and curing time (7 and 28 days), yielding three replicates for each measurement. Consequently, 48 cylindrical specimens were compacted in the field and tested in the laboratory: twenty-four 100 × 200 mm for RM and twenty-four 100 × 100 mm for ITS.

The elastic properties of the materials were investigated through repeated triaxial load tests using a triaxial cell equipped with two external displacement transducers. After curing, the specimens were carefully demoulded, wrapped in a latex membrane and placed in the triaxial cell. Confining and axial stresses were applied via a servo-pneumatic actuator. In accordance with the AASHTO T307 protocol for base/subbase materials [49], each specimen underwent a pre-conditioning phase consisting of 1000 haversine loading pulses, followed by 100 pulses at each of the stress configurations combining different values of major (σ_1) and minor (σ_3) principal stresses. The last five pulses were used to determine the resilient modulus (RM) as the ratio of deviatoric stress ($\sigma_d = \sigma_1 - \sigma_3$) to recoverable axial strain [50]. The RM test outputs were fitted according to the M-EPDG model proposed in the Mechanistic-Empirical Pavement Design Guide [51], to obtain the calibration coefficients that characterise the resilient properties of the material:

$$RM = k_1 \cdot p_a \cdot \left(\frac{I_1}{p_a}\right)^{k_2} \cdot \left(\frac{\tau_{oct}}{p_a} + 1\right)^{k_3} \quad (3)$$

where I_1 is the first stress invariant (i.e., the sum of the three principal stresses), τ_{oct} represents the octahedral shear stress, p_a is the atmospheric pressure, and k_1, k_2, and k_3 are fitting coefficients that vary based on the material properties. In the indirect tensile test, a constant displacement rate of 0.50 mm per minute was applied [52].

Construction of the experimental road

The experimental road was constructed in April 2023 and is 180 m

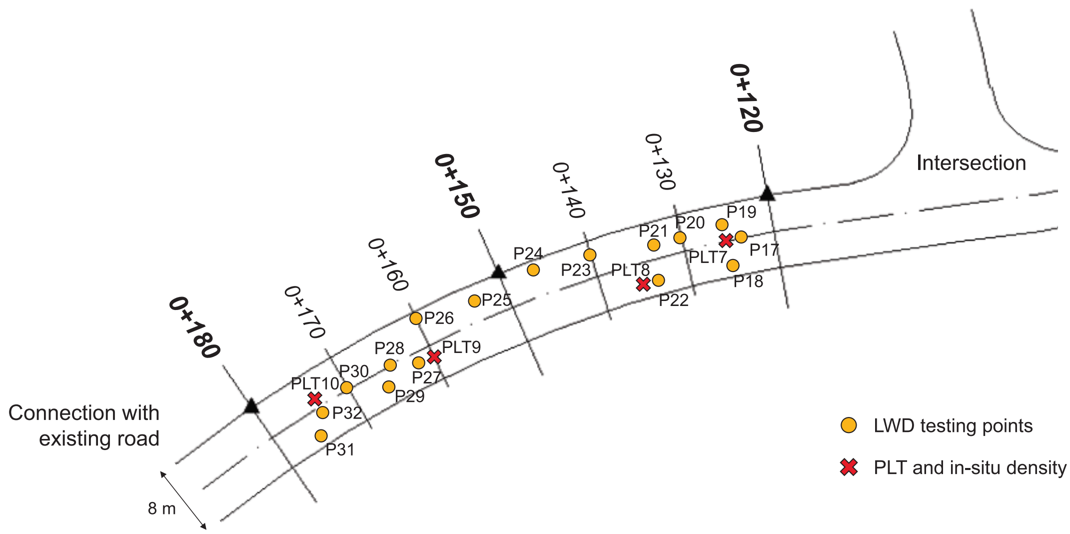

Fig. 6. Map of the testing points of unbound NAT and UCDW subbases.

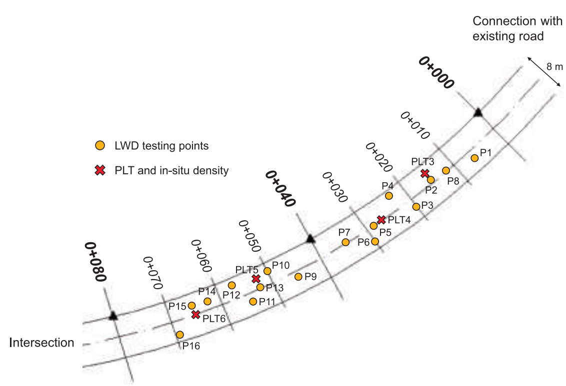

Fig. 7. Map of the testing points of CS-NAT and CS-UCDW subbases.

long and 8 m wide (Fig. 8). The third leg of the intersection corresponds to a low-volume access road for cars only. Heavy trucks follow the main alignment. Moreover, the intersection zone was excluded from testing due to construction complexities and potential compaction issues (Fig. 1). Two 30 m sections were identified for the unbound mixtures and two 40 m sections for the CS subbase formation. Each layer was compacted to achieve the MDD with the corresponding OMC as determined by preliminary laboratory compaction tests.

Subgrade

The subgrade was laid and levelled, then moisturised to achieve the OMC (Table 2), and subsequently laid into two layers of 20 cm each to ensure a more effective roller action during compaction (Fig. 8a). After compaction, twelve LWD (300 mm in diameter) and two plate loading tests were performed along the entire length of the subgrade layer. These tests verified the uniformity of the layer, which serves as support for the upper subbases (see Table 3). As shown in Fig. 9, the testing points were located along the centreline of the 140 m section, while the two PLTs were carried out at stations 0 + 040 m and 0 + 140 m.

The average LWD modulus and standard error of the mean (SEM) were measured as 125.4 ± 9.2 MPa, 129.6 ± 8.6 MPa and 134.2 ± 7.9 MPa for the L, M, and H stress levels, respectively. As expected, the E_{LWD} modulus trend exhibited stress-hardening behaviour [44,53,54]. With coefficients of variation (COV) of 23.0%, 21.0% and 18.5% for the L, M and H stress levels, respectively, it can be concluded that the bearing capacity of the subgrade layer varied within the conventionally set limit of uniformity of construction of 20–25% [55,56]. Furthermore, this variability is largely to be expected given the nature of the test [57,58] and the intrinsic heterogeneity of UCDW materials [59–61].

The PLT indicated a subgrade M_{PLT} ranging from 49.2 to 55.2 MPa and an M'_{PLT} ranging from 207.4 to 279.5 MPa. These results are consistent with the strain moduli measured by Kim and Park [62] on subgrades made with natural aggregate-soil mixtures.

Subbase layers

The unbound subbase layers were formed by laying, levelling, moisturising and compacting the material. Meanwhile, the CS mixtures were produced in a discontinuous mixing plant located next to the experimental road before being laid and compacted (see Fig. 6b). During the mixing process, the aggregates, cement, and water were carefully dosed and mixed for at least three minutes in the mixing chamber. A 20.9-tonne *Dynapac CA6500D* roller was used to compact the unbound and CS layers by vibrating compaction, except for the final static compaction pass, used to create a smooth surface. The number of passes of the roller and the material humidity were adjusted to achieve the MDD. Field tests were carried out on the CS layers after three days of curing. Immediately after compaction, a thin film of bituminous emulsion was sprayed onto the surface to prevent moisture loss and act as a prime coat of the upper bituminous layer. To avoid disturbing the newly placed materials, the construction area was closed to traffic during the curing period. Once the field tests on the sub-bases had been completed, a 10 cm asphalt layer was laid. No further tests were conducted on the final pavement.

Results

Field tests

Tables 4–7 summarise the results of the LWD testing campaign conducted on the four subbases. Each table reports the average values of E_{LWD} calculated from six drops, along with the corresponding standard error (SE), subdivided by the three stress levels indicated in Table 3. The subbase with unbound NAT materials exhibits a uniform behaviour in terms of E_{LWD}, with values ranging from 88.3 to 103.3 MPa for the L stress state, from 94.7 to 109.6 MPa for the M stress level, and from 102.4 to 121.2 MPa for the H stress state. A COV of 5% indicates excellent uniformity in the layer's compaction and mechanical response. The subbase layer containing unbound UCDW exhibited slightly higher average E_{LWD} values than the subbase containing NAT aggregates

Fig. 8. Construction phase: (a) compaction of subgrade, (b) formation of the CS-NAT subbase, (c) preparation of cylindrical samples for laboratory characterisation, and (d) compacted specimen in the plastic split mould.

(Table 5). However, these values were characterised by relatively large spatial variability, consistent with previous studies [48]. In this case, the COV was 11%. The E_{LWD} values were found to range within the following intervals: 97–132 MPa, 103–148 MPa, and 107–152 MPa for the L, M, and H stress levels, respectively. The E_{LWD} values recorded for the CS-NAT (Table 6) and the CS-UCDW (Table 7) subbases are significantly higher than those for the NAT and UCDW unbound aggregate subbase sections. The addition of cement increased the NAT material modulus in the ranges 977–1476 MPa, 947–1327 MPa, and 913–1302 MPa for the L, M and H stress levels, respectively. The COV of 14.4% indicates higher spatial variability in the results. In the CS-UCDW sector, lower moduli than in the CS-NAT subbase were generally observed. Significant spatial variability in the results was observed here, with an average COV of 29.5%. For L, M, and H stress levels, E_{LWD} values were 605–1484 MPa, 570–1407 MPa, and 539–1286 MPa, respectively. The reduction in E_{LWD} observed while increasing the applied stress levels for both the CS-NAT and CS-UCDW materials indicates a mechanical behaviour which is the opposite of that of unbound layers.

The results of the PLT and the sand-cone density tests are presented in Table 8. The unbound NAT and UCDW subbases exhibited very similar behaviour, with M_{PLT} and M'_{PLT} values that were nearly identical. For both unbound subbases, the M_{PLT}/M'_{PLT} ratio was approximately 0.30, indicating a certain degree of additional compaction during testing [48]. The M_{PLT} and M'_{PLT} strain moduli obtained from sectors made up of CS aggregates were significantly higher than those obtained from unbound materials. However, the two points investigated per sector exhibited very different values. For example, in the CS-NAT subbase, the measured values were 978.3 and 391.3 MPa for M_{PLT}, and 1428.6 and 725.8 MPa for M'_{PLT}, respectively. Similarly, the M_{PLT} and M'_{PLT} values for the CS-UCDW subbase differed considerably. The M_{PLT}/M'_{PLT} ratio was higher in cement-stabilised materials than in sectors with unbound material, indicating higher densification of the material during compaction. The in-situ moisture content (MC_{situ}) and dry density (DD_{situ}) during the testing campaign are reported in Table 8. For

Fig. 9. Location of testing points on the subgrade.

Table 4
Average and SEM values of E_{LWD} expressed in MPa of unbound NAT subbase.

Point ID	Stress level (plate diameter = 300 mm)					
	L		M		H	
	Average	SEM	Average	SEM	Average	SEM
P17	95.4	0.6	103.9	0.5	108.1	0.7
P18	97.1	0.7	108.2	0.5	116.0	0.5
P19	89.8	0.5	101.5	0.5	110.1	0.5
P20	88.3	0.5	94.7	0.5	102.4	0.5
P21	101.1	0.9	105.0	0.4	112.5	0.5
P22	94.9	0.7	106.9	0.4	113.7	0.3
P23	91.5	1.0	103.1	0.4	108.7	0.5
P24	103.3	0.4	109.6	0.6	121.2	0.7

Table 5
Average and SEM values of E_{LWD} expressed in MPa of unbound UCDW subbase.

Point ID	Stress level (plate diameter = 300 mm)					
	L		M		H	
	Average	SEM	Average	SEM	Average	SEM
P25	126.0	0.6	125.7	0.6	132.0	0.9
P26	113.3	0.8	121.5	1.1	128.2	0.6
P27	132.3	0.5	147.8	0.5	151.7	0.6
P28	96.8	1.0	113.5	0.6	119.5	0.6
P29	98.1	0.5	102.9	0.3	106.7	0.7
P30	115.8	0.6	119.1	0.5	117.8	1.0
P31	102.9	1.0	109.8	0.6	121.3	1.4
P32	113.3	0.6	128.9	0.7	135.9	1.1

Table 6
Average and SEM values of E_{LWD} in MPa of CS-NAT subbase.

Point ID	Stress level (plate diameter = 200 mm)					
	L		M		H	
	Average	SEM	Average	SEM	Average	SEM
P1	1476.3	25.3	1326.7	13.8	1151.8	12.8
P2	1040.1	11.0	989.5	7.4	976.1	2.8
P3	1366.8	19.3	1278.3	18.2	1207.6	9.4
P4	1096.8	13.4	1017.0	7.9	1016.1	5.0
P5	976.6	12.9	946.6	11.4	912.5	2.7
P6	1083.7	13.7	1011.4	4.9	977.6	5.4
P7	1416.7	16.3	1322.3	8.5	1302.0	7.3
P8	1128.0	11.2	1071.5	7.2	970.6	5.3

Table 7
Average and SEM values of E_{LWD} in MPa of CS-UCDW subbase.

Point ID	Stress level (plate diameter = 200 mm)					
	L		M		H	
	Average	SEM	Average	SEM	Average	SEM
P9	605.2	4.3	595.3	2.4	592.1	2.5
P10	1133.0	17.2	1070.2	5.7	1008.1	1.8
P11	1164.8	14.0	1092.7	8.6	1012.8	3.9
P12	1483.8	15.0	1407.4	11.4	1282.5	13.2
P13	823.8	8.9	765.8	5.7	704.4	7.0
P14	651.6	4.7	570.2	6.0	538.9	2.5
P15	1138.2	9.8	1101.1	3.9	1048.6	4.7
P16	1196.8	22.1	994.7	6.5	890.2	3.9

all subbases, the moisture content fell below the corresponding OMC obtained in the Proctor study. As a result, the DD_{situ} values were consistently lower than the MDD achieved in the laboratory. This deviation from OMC had a uniform effect on all four materials, which explains the consistently lower compaction levels observed across the test sections. It is unlikely that this deviation influenced the comparative trends between the investigated materials.

Laboratory tests

Fig. 10 illustrates the evolution of RM as a function of the first stress invariant (I_1) after 7 and 28 days of curing for the four mixtures. The

Table 8
Results of PLT and sand-cone density test.

Subbase	Testing point	M_{PLT} (MPa)	M'_{PLT} (MPa)	M_{PLT}/M'_{PLT} (–)	MC_{situ} (%)	DD_{situ} (kg/m^3)	DD_{situ}/MDD (%)
NAT	P18	109.8	383.0	0.29	2.2	2090	93.2
	P22	93.5	351.6	0.27	2.8	2018	90.0
UCDW	P27	108.2	367.3	0.29	3.6	2059	96.8
	P32	95.7	311.4	0.31	4.3	1961	92.2
CS-NAT	P2	978.3	1428.6	0.68	4.3	2045	90.7
	P5	391.3	725.8	0.54	4.5	2083	92.4
CS-UCDW	P11	389.6	841.1	0.46	7.5	1984	93.6
	P15	508.5	720.0	0.71	7.5	1914	90.3

values shown represent modelled data derived from fitting the three-repetition experimental data to Eq. (3). Table 9 summarises the fitting parameters and model fitting statistics for all mixtures after 7 and 28 days of curing. The model fitting for all the investigated mixtures is satisfactory, as the coefficients of determination (R^2) are always greater than 0.80 and the SEE/SD ratios are significantly lower than the threshold of 0.55, which defines an unsatisfactory fit (SEE = standard error of the estimate, SD = standard deviation). While the selected indicators are satisfactory, they are not optimal because Eq. (3) was calibrated using the three repetitions. Consequently, they also account for small variations between different samples of the same material.

The coefficient k_1 is proportional to the material stiffness. It is significantly higher in stabilised materials than in unbound ones, which is consistent with the increased stiffness you would expect from the cementitious binding [14]. Furthermore, for the stabilised mixtures, k_1 increases markedly from 7 to 28 days of curing, reflecting the progressive enhancement in the elastic properties of the material. An increase in k_1 during the curing period was also observed for the unbound UCDW material, likely due to self-cementing phenomena associated with the presence of concrete, mortar and cement particles in the UCDW aggregates [67].

Regardless of the material type or curing duration, k_2 is always positive, indicating a stress–hardening behaviour, common to both unbound and cement-stabilised materials whose elastic properties tend to improve with increasing stress levels [68,69].

The coefficient k_3 demonstrated significantly greater variability. For unbound NAT, the sign of k_3 is inverted between 7 and 28 days, indicating a transition from shear-softening to shear-hardening behaviour. For unbound UCDW material, k_3 remains negative, indicating a predominantly shear–softening behaviour [70]. CS mixtures exhibit similar k_3 values for both NAT and UCDW materials. In the case of CS-UCDW cured for 28 days, the close to zero k_3 value suggests that the influence of shear stresses on the resilient behaviour was significantly reduced and limited.

The graphs in Fig. 10 suggest that the unbound NAT specimens cured for 7 days exhibited superior elastic behaviour than the UCDW ones, with significantly higher RM values across the entire I_1 spectrum. After 28 days of curing, the resilient response of the UCDW material improved (Fig. 10a), but the values of RM remained, on average, 24% lower than those of the NAT material (Fig. 10b). As expected, the CS mixtures displayed significantly higher RM values. After 7 days, the CS-UCDW samples (Fig. 10c) exhibited higher stiffness than the corresponding CS-NAT samples (Fig. 10d), with RM values averaging 45% higher. After 28 days of curing, the cement reactions in the CS-NAT mixtures enabled this material to almost match the excellent performance of the CS-UCDW mixtures, albeit the CS-UCDW samples still outperformed, especially at low-to-medium I_1 levels. Both the unbound and CS mixtures exhibited stress hardening, characterised by an increase in RM with increasing stress, which is typical of unbound and CS granular materials.

A parallel tendency in ITS (Fig. 11) was observed between the 7-day-cured CS-NAT and CS-UCDW specimens, with no statistically significant differences ($t_4 = 0.034$, p-value = 0.974). After 28 days of curing, the average ITS value of CS-UCDW was 23% higher than that of CS-NAT, although independent-sample t-tests revealed that this difference was not statistically significant ($t_4 = -1.77$, p-value = 0.152). Increments of 25% and 64% in the average ITS were recorded for the CS-NAT and CS-UCDW mixtures, respectively, when passing from 7 to 28 days ($t_4 = -2.28$, p-value = 0.084 for CS-NAT; $t_4 = -3.07$, p-value = 0.037 for CS-UCDW). In line with the field tests, marked variability in the ITS results was observed for the UCDW aggregates, as indicated by the higher error bars in the bar charts in Fig. 11, representing one standard deviation (SD).

Discussion

Unbound granular materials

The LWD campaign in the two experimental sectors of unbound materials demonstrated the superior bearing capacity of the subbase made with UCDW aggregates compared to that made with NAT ones. This is evident from the higher average E_{LWD} values across all three stress levels (Fig. 12). The high performance of the UCDW material subbases is primarily attributed to their high degree of densification [6,71]. During compaction, UCDW particles (particularly brick, mortar, and weaker concrete fragments) are subjected to compressive and shear stresses from the roller. As widely reported in the literature, this leads to partial fragmentation and a redistribution of particle sizes, creating additional fine material that fills voids and enhances densification [21,63,72]. The statistical analysis supported these experimental findings. The assumptions of normality (Shapiro-Wilk test, W = 0.961, p-value = 0.114) and homogeneity of variance (Levene test, $F_{5,42} = 2.45$, p-value = 0.050) were confirmed, allowing the use of the parametric analysis of variance (ANOVA). The results showed that the type of material (NAT or UCDW) had a significant effect ($F_{1,44} = 32.84$, p-value < 0.001), corroborating the superior bearing capacity of subbases made with unbound UCDW materials compared to those made with NAT aggregates. As shown in Fig. 12, the average E_{LWD} values indicate that both unbound materials exhibited slight stress-hardening behaviour, demonstrating increased mechanical response as vertical stress increased [73,74]. This highlights the influence of stress levels on the estimation of layer moduli using LWD equipment, which is consistent with the stress-dependent evolution observed in the RM of granular materials in the laboratory [75]. ANOVA confirmed that stress levels significantly affected the measured E_{LWD} ($F_{2,44} = 9.67$, p-value < 0.001). Post-hoc comparisons with Holm correction further illustrated this trend, revealing significant differences between L and M stresses (L vs. M, $t_{44} = -2.53$, p-value = 0.030) and between L and H stresses (L vs. H,

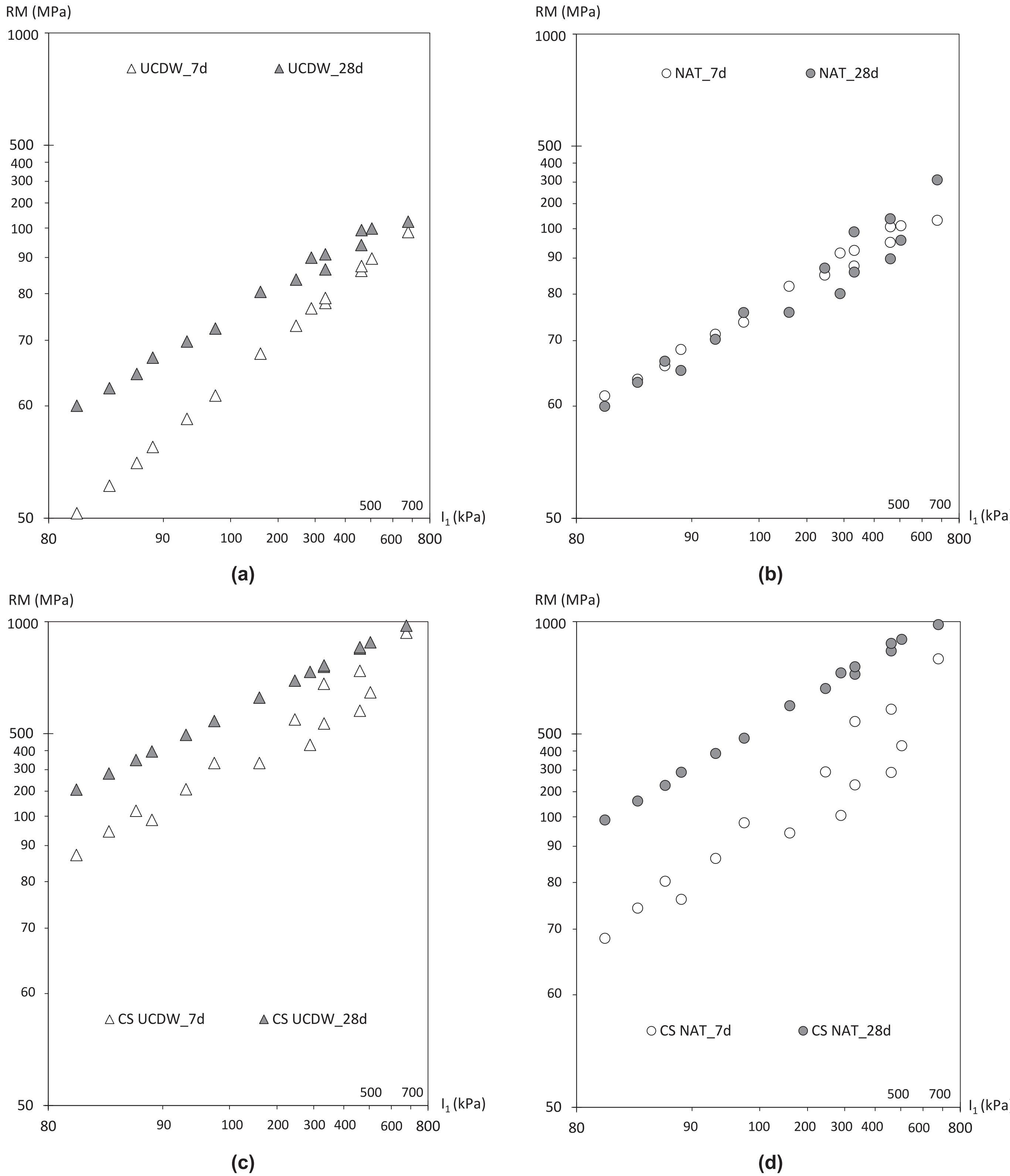

Fig. 10. Resilient modulus results for (a) unbound UCDW, (b) unbound NAT, (c) CS-NAT, and (d) CS-UCDW specimens after 7 and 28 days of curing.

$t_{44} = -4.38$, p–value < 0.001). However, the difference between M and H stress levels was not statistically significant (M vs. H, $t_{44} = -1.85$, p-value $= 0.072$).

In terms of PLT, differences between unbound UCDW and NAT material subbases were not relevant, as equal values of M_{PLT} and M'_{PLT} were measured. The LWD and PLT have different sensitivities to material type because they mobilise different deformation mechanisms. The LWD applies a short-duration impulse load in the upper portion of the layer [76]. In contrast, the PLT transfers a quasi-static load over a deeper influence zone, where the response is governed by the overall compressibility of the compacted layer [77]. Under these conditions, the settlement behaviour of NAT and UCDW is similar, which explains why

Table 9
Regression parameters and model fitting evaluation of RM test results by the M-EPDG model. SEE/SD is the ratio between the standard error of estimate (SEE) and the standard deviation of measure data (SD). It represents the goodness-of-fit variable as "excellent" for SEE/SD ≤ 0.35, "good" for.36 ≤ SEE/SD ≤ 0.55, "fair" for.56 ≤ SEE/SD ≤ 0.75, and "poor" for.76 ≤ SEE/SD ≤ 0.90 [57].

Material	Curing	M-EPDG model parameters			Statistics of the model fitting	
		k_1	k_2	k_3	R^2	SEE/SD
Unbound NAT	7 d	1135	0.67	−0.34	0.84	0.42
	28 d	932	0.38	0.89	0.86	0.41
Unbound UCDW	7 d	546	0.91	−0.11	0.92	0.30
	28 d	1066	0.69	−0.33	0.93	0.27
CS-NAT	7 d	1261	0.35	1.39	0.85	0.40
	28 d	3079	0.66	−0.16	0.92	0.29
CS-UCDW	7 d	2201	0.37	0.88	0.82	0.44
	28 d	3623	0.52	−0.03	0.96	0.19

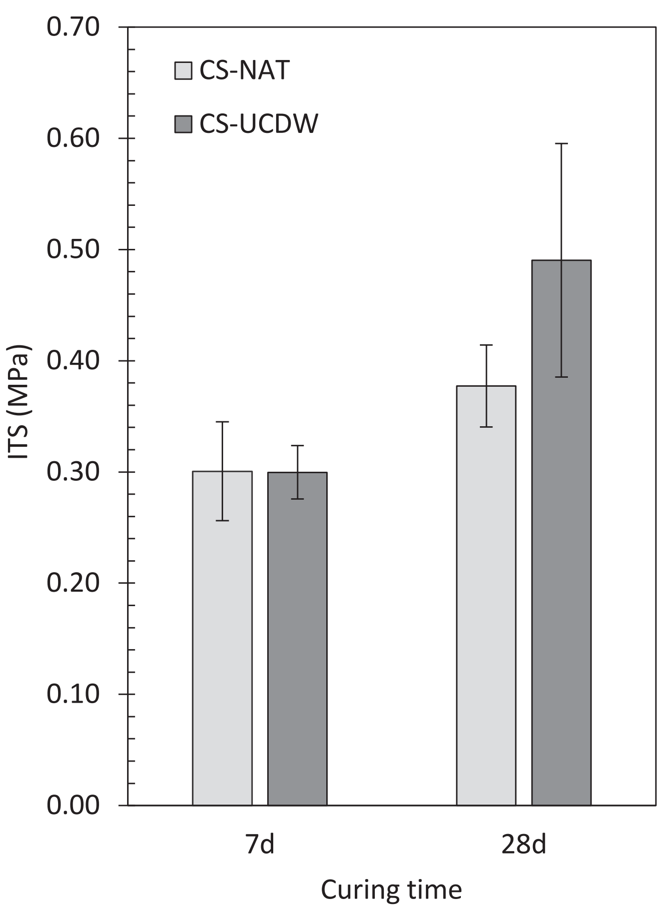

Fig. 11. Average ITS results of CS-NAT, and CS-UCDW specimens after 7 and 28 days of curing. The error bars indicate one SD.

the differences observed in PLT moduli are smaller than those observed in LWD characterisation. It should also be noted that the bearing capacity results obtained using PLT on unbound subbases are consistent with the results of previous studies [29]. These results confirm the validity of using compacted UCDW as an alternative to natural and virgin materials in the construction of unbound subbases, consistent with previous studies [3,14,78,79].

Laboratory tests carried out after 7 and 28 days indicated a slightly

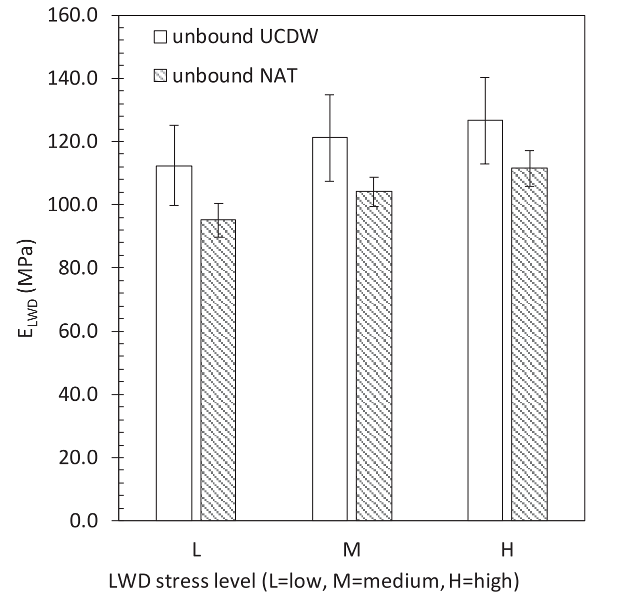

Fig. 12. Average E_{LWD} moduli across the unbound NAT and UCDW subbase sectors for L, M, and H LWD stress levels. Error bars indicate one SD.

higher ITS in the UCDW samples than in the NAT samples. The higher strength properties of UCDW are due to self-cementing phenomena resulting from the reaction of cement particles with the addition of water, as observed by [80,81].

In contrast, repeated load triaxial tests showed that the RM of the NAT aggregate was significantly higher than that of the UCDW aggregate across the entire stress spectrum investigated.

The observed difference between E_{LWD} field measurements and laboratory RM values for NAT and UCDW aggregates can be attributed to several factors. In contrast to laboratory testing, field tests are influenced by environmental conditions, limitations in controlling material handling, compaction procedures, and the uniform addition and distribution of water into granular masses. It is important to note that variations in moisture content significantly affect compaction efficiency and the resulting stress–strain response of the granular material [82–84]. It is likely that the observed discrepancies between field and laboratory stiffness measurements for the two aggregates are primarily due to differences in moisture conditions, as indicated by the lower amount of water (MC_{situ}, Table 8) in the unbound materials (both NAT and UCDW) with respect to the OMC (Table 2). Anyway, the RM values of the UCDW and NAT materials are consistent with literature data [3,85,86]. As the curing time increased to 28 days, the differences between the unbound NAT and UCDW materials decreased, resulting in comparable RM values, particularly at higher I_1 stress invariants. The time-dependent increase in stiffness of the UCDW mixture corroborates the assumption of self-cementing phenomena occurring in the materials that create bonds between particles [67].

Although the unbound UCDW material exhibited an excellent response under loading, it also generated greater variability than the NAT material in both field and laboratory tests. The heterogeneous composition of UCDW has been identified as the primary cause of this dispersion in results [87,88].

Cement-stabilised materials

The mechanical properties of CS subbases were markedly higher than those of unbound subbases, thus demonstrating the effectiveness of adding cement to NAT and UCDW aggregates. During the LWD campaign, the average E_{LWD} recorded for CS mixtures at the M stress level was approximately eight to ten times greater than that for unbound NAT and UCDW, respectively (Fig. 13). In contrast to unbound mixtures,

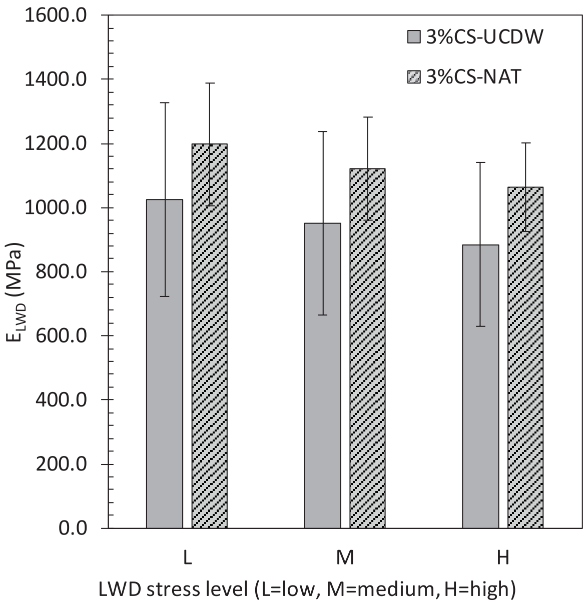

Fig. 13. Average E_{LWD} moduli across the cement-stabilised NAT and UCDW subbase sectors for L, M, and H LWD stress levels. Error bars indicate one SD.

the subbase consisting of CS-NAT had a higher average E_{LWD} than the subbase consisting of CS-UCDW at all three stress levels. The binding phase plays a crucial role in transferring loads to the aggregate skeleton [89,90]. In the case of NAT aggregates, the hardened, non-deformable structure can resist external loads. In contrast, the weaker UCDW particles tend to fracture under repeated loading, reducing the overall mechanical properties of the subbase [91,92]. It is also worth noting that the density of the CS-UCDW layer (Table 8) was slightly lower than the MDD of the Proctor test, which partly contributed to its inferior mechanical properties [93].

These results were corroborated by ANOVA (Shapiro-Wilk test, $W = 0.967$, p-value $= 0.197$; Levene, $F_{5,42} = 1.80$, p-value $= 0.134$). The effect of the material type (CS-UCDW vs. CS-NAT) on E_{LWD} values was found to be statistically significant ($F_{1,44} = 7.19$, p-value $= 0.010$), confirming that the CS-NAT subbase provided an overall higher bearing capacity than the CS-UCDW subbase.

Stress-softening behaviour was exhibited by both CS subbases, with E_{LWD} decreasing as the vertical load increased from the L to the H stress level. This behaviour contrasts with the stress-hardening responses typically observed in laboratory RM tests (see Fig. 10). It is supposed that during the LWD test, the stiff, dry surface layer (within the first few centimetres beneath the plate) underwent localised microcracking in the drop zone [94]. As the number of drops increased, these microcracks led to greater strain on impact, reducing the measured E_{LWD} values [95]. However, the effect of stress levels, as evaluated by ANOVA, was not significant ($F_{2,44} = 1.48$, p-value $= 0.239$), indicating that the observed decrease in E_{LWD} from L to H stress levels (i.e., the stress-softening behaviour) was not statistically significant across the dataset [96].

In addition, significant spatial variability was observed across the sector for both the CS-NAT and CS-UCDW subbases, as is commonly documented in LWD investigations [49,97,98]. In this field study, various factors could have contributed to this. Although the CS mixtures were prepared by uniformly mixing aggregates, cement, and water, discrepancies in moisture content can occur along the testing sections. This directly affects the hydration reaction of the cement, resulting in different LWD responses. The variability is even more pronounced in the CS-UCDW material due to its heterogeneous nature. Furthermore, high COV values can indicate an inadequate distribution of water in the mixture for cement hydration processes [99], primarily due to significant variation in the water absorption capacities of the constituent materials [100].

In contrast to the field test results, laboratory results showed that CS-UCDW specimens had superior mechanical performance to CS-NAT specimens. After 7 days of curing, CS-UCDW mixtures exhibited significantly higher RM values than CS-NAT mixtures did. The RM values recorded for 7-day cured CS-NAT specimens are lower than those previously reported in [3], whereas the RM of 7-day cured CS-UCDW material aligns with that reported in previous studies [3,57,58]. However, after 28 days of curing, the RM of the CS-NAT material increased considerably, almost reaching the excellent resilient properties of the CS-UCDW mixture.

Finally, the addition of cement significantly increased the strength of both the NAT and the UCDW mixtures in the indirect tensile tests, as evidenced by the higher average values shown in Fig. 11. The formation of weak bonds between grains enables the materials to withstand tensile stresses in the diametral area zone of the specimen. Notably, both CS-NAT and CS-UCDW mixtures exhibited ITS values significantly above the 0.250 MPa threshold required by the Italian Technical Specifications [32] for CS materials used in road subbases after 7 days of curing.

Implications

There is no reason to believe that unbound and CS-UCDW aggregate cannot be used as a substitute for traditional materials containing virgin NAT aggregates. The load-bearing capacity of recycled materials is comparable to, and often exceeds, that of traditional materials still widely used in road subbase construction today. In Italy, the supply of UCDW aggregates is abundant, as national recycling rates are high and in line with European trends [101]. Despite this, their use in pavement construction has so far been limited, with most applications confined to subgrades and support layers for industrial platforms. Although recycling plants are generally equipped to produce high-quality UCDW through controlled sorting and cleaning processes, concerns regarding variability have historically reduced industry confidence [102]. However, recent regulatory developments, including the introduction of Minimum Environmental Criteria for roadworks, now require contractors to use minimum percentages of recycled materials. Several road authorities are also beginning to adapt their technical specifications accordingly. These policy changes are expected to substantially increase the practical use of UCDW in pavement subbase applications.

The results of this study should convince even the most sceptical individuals that using UCDW in subbase pavement layers is possible and, indeed, cost- and environmentally effective. They should also serve to persuade technicians and legislators to set a minimum threshold of close to, if not equal to, 100% for UCDW materials in pavement subbases.

However, the compositions of UCDW aggregates are highly variable, and this variance is transmitted to the physical and mechanical properties of the structures that include them. It is this intrinsic variability in properties that differentiates the performance of recycled aggregates from that of natural ones. Therefore, careful consideration must be given to the bearing capacity values used in pavement analysis and design, bearing in mind the non-normal nature of the surface modulus values observed in this study. It is also worth noting that variability in physical and mechanical properties can be reduced during production by controlling the composition of waste entering recycling plants or by promoting the mixing of larger volumes of individual size classes before use on construction sites.

Limitations and future needs

The experimental design of this study aimed to minimise the number of factors that affect variability in the results and to simplify their interpretation. However, this restricts the generalisability of the results, which can only be achieved through a new experimental design that modifies these factors and their levels of variation.

Although the cement content is a key parameter in controlling the mechanical properties, environmental impact, and economic aspects of the mixture, only a single dosage of 3% by dry mass was investigated due to logistical and economic constraints. From a sustainability perspective, increasing the cement content generally increases embodied impacts, so identifying the minimum dosage that meets structural and durability requirements is essential. Future work should therefore combine mechanical testing with environmental assessments and sensitivity analyses of cement dosage and binder type.

The quality and type of waste converted into aggregate strongly influence all experiments on recycled materials. Further studies on UCDW aggregates in different contexts could expand our understanding of this area. Although UCDW materials are inherently heterogeneous, the composition measured in this study is consistent with that observed in previous studies. Consistent trends observed across numerous field and laboratory repetitions suggest that the findings are representative of commonly encountered UCDW aggregates. However, future investigations involving different recycling plants, regional waste streams and production conditions would enhance the applicability of the results. Aspects of durability, such as wetting and drying or freeze–thaw cycling, as well as the long-term degradation of recycled aggregates, were not included in this study and should be addressed in future research to complement these findings.

Using the LWD to assess the mechanical properties of road subbases revealed persistent spatial variability in the results, particularly for cement-stabilised materials. Selecting points across the entire section to be tested is critical for an accurate assessment. However, because the LWD test is quite fast, the number of test points can be increased to obtain a more comprehensive and reliable indication of the layer's response across its entire extent. Nevertheless, further research efforts should minimise measurement variability and ensure consistent results, particularly with UCDW aggregates.

Conclusion

This research aimed to evaluate and compare the bearing capacity of road subbases composed of natural (NAT) aggregate and unselected construction and demolition waste (UCDW) aggregate. To this end, an experimental road was constructed with 30 cm-thick subbases comprising four sections: (i) unbound NAT aggregate, (ii) unbound UCDW aggregate, (iii) cement-stabilised (CS) NAT material, and (iv) CS-UCDW aggregate. A Light Weight Deflectometer (LWD) test campaign was conducted 3 days after laying and compaction. In parallel, resilient modulus and indirect tensile strength tests were performed on specimens prepared with the same materials at the construction site and cured under controlled conditions (25 °C and RH > 90%) for 7 and 28 days.

Field investigations revealed that unbound UCDW materials outperform NAT aggregates in subbase applications. On average, the bearing capacity of subbases made of unbound UCDW is 16% higher than that of subbases made of NAT aggregates. The UCDW materials contain cement and concrete particles with self-cementing properties that are activated by adding water and subsequent compaction, producing a denser, stiffer material. Laboratory tests corroborated these findings, showing an average increase in stiffness of 29% for UCDW aggregates when passing from 7 to 28 days of curing.

The investigation also compared CS mixtures made using aggregates from the two sources (NAT and UCDW). Adding 3% cement and 8.5% water increased the bearing capacity of both NAT and UCDW aggregates by factors of 10 and 7, respectively. While the CS-NAT mixture performed better than the CS-UCDW mixture in field tests after 3 days of curing, the laboratory investigation performed on 7 and 28-day cured specimens produced an inverse result, with the CS-UCDW mixture outperforming the CS-NAT mixture, particularly in the low-to-medium stress domain of the resilient modulus test protocol. While the subbase containing CS-NAT had a higher bearing capacity than the corresponding subbase with UCDW material, it is reasonable to suspect that the difference in field performance between the two materials would dissipate over a longer curing time.

The use of the LWD equipment with different loading configurations enables the stress-dependent behaviour of unbound and CS granular materials to be evaluated. It was found that unbound mixtures tended to exhibit stress-hardening behaviour, with the modulus increasing as the transmitted vertical stress rose. Contrary to expectations, both CS-NAT and CS-UCDW mixtures exhibited a stress-softening response under loading. As is often the case with UCDW materials, considerable spatial variability in the surface modulus was observed in both unbound and stabilised UCDW mixtures, due to the heterogeneous nature of this waste source.

CRediT authorship contribution statement

Luca Tefa: Writing – review & editing, Writing – original draft, Visualization, Software, Methodology, Investigation, Formal analysis, Data curation, Conceptualization. **Marco Bassani:** Writing – review & editing, Writing – original draft, Validation, Supervision, Resources, Project administration, Methodology, Investigation, Funding acquisition, Formal analysis, Conceptualization.

Declaration of competing interest

The authors declare that they have no known competing financial interests or personal relationships that could have appeared to influence the work reported in this paper.

Acknowledgements

This research is part of the INTREC project, which was funded by the Regione Piemonte (Italy) through the EU Regional Development Fund (P.O.R. FESR 2014–2020, Asse I, Azione I.1b.1.2, PRISM-E). The authors would like to thank Cavit S.p.A. for providing the facilities and equipment used to produce the materials and construct the experimental road. Special thanks go to Fadil Kërtusha, who conducted most of the field and laboratory tests, and to Alberto Portera and Alessandra Lioi, who provided invaluable support for field activities.

Data availability

Data will be made available on request.

References

[1] Pereira HDM, Bessa Júnior JE, Nóbrega RADA. Geospatial-based decision support system for prioritizing road segments for maintenance and rehabilitation. Case Stud Transp Policy 2024;16:101170. https://doi.org/10.1016/j.cstp.2024.101170.

[2] Daulat S, Rokstad MM, Klein-Paste A, Langeveld J, Tscheikner-Gratl F. Challenges of integrated multi-infrastructure asset management: a review of pavement, sewer, and water distribution networks. Struct Infrastruct Eng 2024;20:546–65. https://doi.org/10.1080/15732479.2022.2119480.

[3] Tefa L, Bianco I, Blengini GA, Bassani M. Integrated and comparative Structural-LCA analysis of unbound and cement-stabilized construction and demolition waste aggregate for subbase road pavement layers formation. J Clean Prod 2022;352:131599. https://doi.org/10.1016/j.jclepro.2022.131599.

[4] Menegaki M, Damigos D. A review on current situation and challenges of construction and demolition waste management. Curr Opin Green Sustainable Chem 2018;13:8–15. https://doi.org/10.1016/j.cogsc.2018.02.010.

[5] Eurostat, Waste statistics – Statistics Explained; 2024. https://ec.europa.eu/eurostat/statistics-explained/index.php?title=Waste_statistics.

[6] Bassani M, Tefa L. Compaction and freeze-thaw degradation assessment of recycled aggregates from unseparated construction and demolition waste. Constr Build Mater 2018;160:180–95. https://doi.org/10.1016/j.conbuildmat.2017.11.052.

[7] Jiménez JR. Recycled aggregates (RAs) for roads. In: Handbook of recycled concrete and demolition waste. Elsevier; 2013. p. 351–77. https://doi.org/10.1533/9780857096906.3.351.

[8] Silva RV, de Brito J, Dhir RK. Availability and processing of recycled aggregates within the construction and demolition supply chain: a review. J Clean Prod 2017;143:598–614. https://doi.org/10.1016/j.jclepro.2016.12.070.

[9] Verian KP, Ashraf W, Cao Y. Properties of recycled concrete aggregate and their influence in new concrete production. Resour Conserv Recycl 2018;133:30–49. https://doi.org/10.1016/j.resconrec.2018.02.005.
[10] Mariyappan R, Palammal JS, Balu S. Sustainable use of reclaimed asphalt pavement (RAP) in pavement applications—a review. Environ Sci Pollut Res 2023;30:45587–606. https://doi.org/10.1007/s11356-023-25847-3.
[11] Galán B, Viguri JR, Cifrian E, Dosal E, Andres A. Influence of input streams on the construction and demolition waste (CDW) recycling performance of basic and advanced treatment plants. J Clean Prod 2019;236:117523. https://doi.org/10.1016/j.jclepro.2019.06.354.
[12] Zhao Y, Goulias D, Tefa L, Bassani M. Life cycle economic and environmental impacts of CDW recycled aggregates in roadway construction and rehabilitation. Sustainability 2021;13:8611. https://doi.org/10.3390/su13158611.
[13] Cardoso R, Silva RV, de Brito J, Dhir R. Use of recycled aggregates from construction and demolition waste in geotechnical applications: a literature review. Waste Manag 2016;49:131–45. https://doi.org/10.1016/j.wasman.2015.12.021.
[14] Corradini A, Cerni G, Porceddu PR. Comparative study on resilient modulus of natural and post-quake recycled aggregates in bound and unbound pavement subbase applications. Constr Build Mater 2021;297:123717. https://doi.org/10.1016/j.conbuildmat.2021.123717.
[15] Jiménez JR, Ayuso J, Galvín AP, López M, Agrela F. Use of mixed recycled aggregates with a low embodied energy from non-selected CDW in unpaved rural roads. Constr Build Mater 2012;34:34–43. https://doi.org/10.1016/j.conbuildmat.2012.02.042.
[16] Tavakoli Mehrjardi G, Azizi A, Haji-Azizi A, Asdollafardi G. Evaluating and improving the construction and demolition waste technical properties to use in road construction. Transp Geotech 2020;23:100349. https://doi.org/10.1016/j.trgeo.2020.100349.
[17] Mallick RB, El-Korchi T. Pavement engineering: principles and practice. 2nd ed. Boca Raton (FL): CRC Press; 2013.
[18] Marek CR. Compaction of graded aggregate bases and subbases. Transp Eng J ASCE 1977;103:103–13. https://doi.org/10.1061/TPEJAN.0000611.
[19] Xiao Y, Tutumluer E, Qian Y, Siekmeier JA. Gradation effects influencing mechanical properties of aggregate base–granular subbase materials in Minnesota. Transp Res Rec 2012;2267:14–26. https://doi.org/10.3141/2267-02.
[20] Abedin Khan Z, Balunaini U, Costa S, Nguyen NHT. A review on sustainable use of recycled construction and demolition waste aggregates in pavement base and subbase layers. Cleaner Mater 2024;13:100266. https://doi.org/10.1016/j.clema.2024.100266.
[21] Brito Da Silva T, De Souza Correia N, De Oliveira Kühn V. Effect of compaction energy on grain breakage of CDW, local soil and soil-CDW mixtures. Int J Geotech Eng 2022;16:165–75. https://doi.org/10.1080/19386362.2021.1932311.
[22] Marik S, Ransinchung GD, Singh RNA, Khot LP. Laboratory study and performance evaluation of cement treated base using chemical stabiliser. Road Mater Pavement Des 2023;24:1522–41. https://doi.org/10.1080/14680629.2022.2083660.
[23] Arulrajah A, Mohammadinia A, Haghighi H, Horpibulsuk S. Effect of moisture sensitivity on the light stabilisation of demolition materials in pavement bases. Road Mater Pavement Des 2022;23:787–801. https://doi.org/10.1080/14680629.2020.1843525.
[24] Kulkarni PP, Mandal JN. Strength evaluation of soil stabilized with nano silica-cement mixes as road construction material. Constr Build Mater 2022;314:125363. https://doi.org/10.1016/j.conbuildmat.2021.125363.
[25] Park T. Application of construction and building debris as base and subbase materials in rigid pavement. J Transp Eng 2003;129(5):558–63. https://doi.org/10.1061/(ASCE)0733-947X(2003)129:5(558).
[26] Pérez P, Agrela F, Herrador R, Ordoñez J. Application of cement-treated recycled materials in the construction of a section of road in Malaga, Spain. Constr Build Mater 2013;44:593–9. https://doi.org/10.1016/j.conbuildmat.2013.02.034.
[27] Isola M, Betti G, Marradi A, Tebaldi G. Evaluation of cement treated mixtures with high percentage of reclaimed asphalt pavement. Constr Build Mater 2013;48:238–47. https://doi.org/10.1016/j.conbuildmat.2013.06.042.
[28] Pereira PM, Vieira CS. A literature review on the use of recycled construction and demolition materials in unbound pavement applications. Sustainability 2022;14:13918. https://doi.org/10.3390/su142113918.
[29] Tavira J, Jiménez JR, Ayuso J, Sierra MJ, Ledesma EF. Functional and structural parameters of a paved road section constructed with mixed recycled aggregates from non-selected construction and demolition waste with excavation soil. Constr Build Mater 2018;164:57–69. https://doi.org/10.1016/j.conbuildmat.2017.12.195.
[30] Beja IA, Motta R, Bernucci LB. Application of recycled aggregates from construction and demolition waste with Portland cement and hydrated lime as pavement subbase in Brazil. Constr Build Mater 2020;258:119520. https://doi.org/10.1016/j.conbuildmat.2020.119520.
[31] Nunn ME, Brown A, Weston D, Nicholls JC. Design of long-life flexible pavements for heavy traffic. Crowthorne, UK: Transport Research Foundation Group of Companies; 1997 [accessed August 19, 2025], https://trid.trb.org/View/475038.
[32] Centro Sperimentale Interuniversitario di Ricerca Stradale, Studio a carattere pre-normativo delle norme tecniche di tipo prestazionale per capitolati speciali d'appalto; 2001.
[33] Domenichini L, Di Mascio P, Giannattasio P, Caliendo C, Festa B, Marchionna A, et al. Modello di catalogo delle pavimentazioni stradali. Rome (Italy): Permanent International Association of Road Congresses; 1995.
[34] European Committee for Standardization. Tests for geometrical properties of aggregates – Part 1: Determination of particle size distribution – Sieving method; 2012.
[35] European Committee for Standardization. Unbound and hydraulically bound mixtures – Part 2: Test methods for laboratory reference density and water content – proctor compaction; 2010.
[36] Tefa L, Bianco I, Bassani M. Stabilising CDW recycled aggregates with alternatives to Portland cement. Constr Build Mater 2025;471:140705. https://doi.org/10.1016/j.conbuildmat.2025.140705.
[37] Nazari Z, Tabarsa A, Latifi N. Effect of compaction delay on the strength and consolidation properties of cement-stabilized subgrade soil. Transp Geotech 2021;27:100495. https://doi.org/10.1016/j.trgeo.2020.100495.
[38] Santagata FA. Strade – Teoria e tecnica delle costruzioni stradali. Torino: Pearson; 2016.
[39] Ridolfi S, Garbin F. Geologia e geotecnica stradale – I materiali e la loro caratterizzazione. Palermo (Italy): Dario Flaccovio Editore; 2010.
[40] Tefa L, Bassani M. Deliverable WP1 – INTREC project (Innovative Technologies for Recycled Aggregates from Construction and Demolition Waste in Road Constructions), Turin, Italy; 2021.
[41] European Committee for Standardization, Cement – Part 1: Composition, specifications and conformity criteria for common cements; 2011.
[42] American Society for Testing and Materials. Standard test method for measuring deflections with a light weight deflectometer (LWD); 2007.
[43] Edwards P, Fleming P. LWD best practice guide. Loughborough (UK): Loughborough University; 2012.
[44] Tefa L, Bassani M. Stress dependent behaviour of unbound layers of unselected construction and demolition waste aggregates by lightweight deflectometer tests. Eur Transp/Trasporti Europe 2023;91. https://doi.org/10.48295/ET.2023.91.7.
[45] Fleming PR, Frost MW, Lambert JP. Review of lightweight deflectometer for routine in situ assessment of pavement material stiffness. Transp Res Rec 2004;2007:80–7. https://doi.org/10.3141/2004-09.
[46] Ullidtz P. Modelling flexible pavement response and performance. Lyngby (Denmark): Tech Univ. of Denmark Polyteknisk Forlag; 1998.
[47] Consiglio Nazionale delle Ricerche (CNR). Determinazione del moduli di deformazione Md e M'd mediante prova di carico a doppio ciclo con piastra circolare; 1992.
[48] American Society for Testing and Materials. Standard test method for density and unit weight of soil in place by sand-cone method; 2015.
[49] American Association of State and Highway Transportation Officials. Standard method of test for determining the resilient modulus of soils and aggregate materials; 2013.
[50] Lekarp F, Isacsson U, Dawson A. State of the art. II: Permanent strain response of unbound aggregates. J Transp Eng 2000;126:76–83. https://doi.org/10.1061/(ASCE)0733-947X(2000)126:1(76).
[51] American Association of State Highway and Transportation Officials. Mechanistic-empirical pavement design guide: a manual of practice. Washington, DC: American Association of State Highway and Transportation Officials; 2008.
[52] Hudson WR, Kennedy TW. An indirect tensile test for stabilized materials. Austin (TX, U.S.): Center for Highway Research, University of Texas at Austin; 1968.
[53] Luo X, Liu G, Zhang Y, Meng T, Zhan L. Estimation of resilient modulus of cement-treated construction and demolition waste with performance-related properties. Constr Build Mater 2021;283:122107. https://doi.org/10.1016/j.conbuildmat.2020.122107.
[54] Bassani M, Riviera PP, Tefa L. Short-term and long-term effects of cement kiln dust stabilization of construction and demolition waste. J Mater Civ Eng 2017;29:04016286. https://doi.org/10.1061/(ASCE)MT.1943-5533.0001797.
[55] Bakare MD, Shahu JT, Patel S. Complete substitution of natural aggregates with industrial wastes in road subbase: a field study. Resour Conserv Recycl 2023;190:106856. https://doi.org/10.1016/j.resconrec.2022.106856.
[56] Duddu SR, Kommanamanchi V, Chennarapu H, Mahopatra PK. In-situ assessment of dynamic deformation modulus of pavement layers using light weight deflectometer. Transp Infrastruct Geotech 2024;11:2023–45. https://doi.org/10.1007/s40515-023-00359-2.
[57] Mazari M, Garcia G, Abdallah I, Garibay J, Nazarian S. Variability of light weight deflectometer during laboratory and field applications for subgrade soils under variable moisture conditions. Bearing capacity of roads, railways and airfields. CRC Press; 2017.
[58] Garcia VM, Robinson J. Application of lightweight deflectometer to assess structural competency of nontraditional airfield pavements during contingency aircraft operations. Transp Res Rec 2023;2679(1):332–45. https://doi.org/10.1177/03611981231153644.
[59] Leite F da C, Motta R dos S, Vasconcelos KL, Bernucci L. Laboratory evaluation of recycled construction and demolition waste for pavements. Constr Build Mater 2011;25:2972–9. https://doi.org/10.1016/j.conbuildmat.2010.11.105.
[60] Islam R, Nazifa TH, Yuniarto A, Shanawaz Uddin ASM, Salmiati S, Shahid S. An empirical study of construction and demolition waste generation and implication of recycling. Waste Manag 2019;95:10–21. https://doi.org/10.1016/j.wasman.2019.05.049.
[61] S B, D R, C.W.W N. Feasibility of construction demolition waste for unexplored geotechnical and geo-environmental applications – a review. Constr Build Mater 2022;356:129230. https://doi.org/10.1016/j.conbuildmat.2022.129230.
[62] Kim D, Park S. Relationship between the subgrade reaction modulus and the strain modulus obtained using a plate loading test. 9th world congress on railway research, Lille, France. 2011.
[63] Wang C, Chazallon C, Hornych P, Mouhoubi S, Jing P. Effect of self-cementing properties on the resilient behaviour of recycled concrete aggregates used in base

and subbase. Road Mater Pavement Des 2024:1–17. https://doi.org/10.1080/14680629.2024.2302804.
[64] Lekarp F, Isacsson U, Dawson A. State of the art. I: Resilient response of unbound aggregates. J Transp Eng 2000;126(1):66–75. https://doi.org/10.1061/(ASCE)0733-947X(2000)126:1(66).
[65] Puppala AJ, Hoyos LR, Potturi AK. Resilient moduli response of moderately cement-treated reclaimed asphalt pavement aggregates. J Mater Civ Eng 2011;23:990–8.
[66] Hanifa K, Abu-Farsakh MY, Gautreau GP. Design values of resilient modulus for stabilized and non-stabilized base. Baton Rouge (LA): Louisiana Transportation Research Center; 2015.
[67] John NJ, Khan I, Patel A. Evaluation of the crushing characteristics of industrial waste aggregates as construction materials. Constr Build Mater 2023;403:133111. https://doi.org/10.1016/j.conbuildmat.2023.133111.
[68] Xu Y. Fractal dimension of demolition waste fragmentation and its implication of compactness. Powder Technol 2018;339:922–9. https://doi.org/10.1016/j.powtec.2018.08.071.
[69] Sabouri M, Khabiri S, Asgharzadeh SM, Abdollahi SF. Investigating the performance of geogrid reinforced unbound layer using light weight deflectometer (LWD). Int J Pavement Res Technol 2022;15:173–83. https://doi.org/10.1007/s42947-021-00015-3.
[70] Kavussi A, Qorbaninik M, Hassani A. The influence of moisture content and compaction level on LWD modulus of unbound granular base layers. Transp Geotech 2019;20:100252. https://doi.org/10.1016/j.trgeo.2019.100252.
[71] Jones RH, Dawson AR, editors. Unbound aggregates in roads. Butterworths, London, Boston; 1989.
[72] Tawfik MM, El-Mossallamy YM. Application of the finite element method for investigating the dynamic plate loading test. Ain Shams Eng J 2017;8:39–49. https://doi.org/10.1016/j.asej.2015.08.011.
[73] Decký M, Drusa M, Papán D, Šrámek J. The relationship between dynamic and static deformation modulus of unbound pavement materials used for their quality control methodology. Materials 2022;15:2922. https://doi.org/10.3390/ma15082922.
[74] Ossa A, García JL, Botero E. Use of recycled construction and demolition waste (CDW) aggregates: a sustainable alternative for the pavement construction industry. J Clean Prod 2016;135:379–86. https://doi.org/10.1016/j.jclepro.2016.06.088.
[75] Esfahani MA. Evaluating the feasibility, usability, and strength of recycled construction and demolition waste in base and subbase courses. Road Mater Pavement Des 2020;21:156–78. https://doi.org/10.1080/14680629.2018.1483259.
[76] Arm M. Self-cementing properties of crushed demolished concrete in unbound layers: results from triaxial tests and field tests. Waste Manag 2001;21:235–9. https://doi.org/10.1016/S0956-053X(00)00095-7.
[77] Martinez-Echevarria MJ, Lopez-Alonso M, Garach L, Alegre J, Poon CS, Agrela F, et al. Crushing treatment on recycled aggregates to improve their mechanical behaviour for use in unbound road layers. Constr Build Mater 2020;263:120517. https://doi.org/10.1016/j.conbuildmat.2020.120517.
[78] Thai HN, Nguyen TD, Nguyen VT, Nguyen HG, Kawamoto K. Characterization of compaction and CBR properties of recycled concrete aggregates for unbound road base and subbase materials in Vietnam. J Mater Cycles Waste Manag 2022;24:34–48. https://doi.org/10.1007/s10163-021-01333-1.
[79] Hu W, Jia X, Zhu X, Su A, Du Y, Huang B. Influence of moisture content on intelligent soil compaction. Autom Constr 2020;113:103141. https://doi.org/10.1016/j.autcon.2020.103141.
[80] Chen D-H, Zaman M, Laguros J. Characterization of base/subbase materials under repetitive loading. J Test Eval 1995;23:180–8. https://doi.org/10.1520/JTE10408J.
[81] Bennert MT, Maher DA. The development of a performance specification for granular base and subbase material. Trenton (NJ): New Jersey Department of Transportation; n.d.
[82] Saeed A. Performance-related tests of recycled aggregates for use in unbound pavement layers. Washington, DC: Transportation Research Board; 2008. https://doi.org/10.17226/23108.
[83] Barbudo A, Agrela F, Ayuso J, Jiménez JR, Poon CS. Statistical analysis of recycled aggregates derived from different sources for sub-base applications. Constr Build Mater 2012;28:129–38. https://doi.org/10.1016/j.conbuildmat.2011.07.035.
[84] Delongui L, Matuella M, Núñez WP, Fedrigo W, da Silva Filho LCP, Ceratti JAP. Construction and demolition waste parameters for rational pavement design. Constr Build Mater 2018;168:105–12. https://doi.org/10.1016/j.conbuildmat.2018.02.086.
[85] Guotang Z, Wei S, Guotao Y, Li P, Degou C, Jinyang J, et al. Mechanism of cement on the performance of cement stabilized aggregate for high speed railway roadbed. Constr Build Mater 2017;144:347–56. https://doi.org/10.1016/j.conbuildmat.2017.03.194.
[86] Halsted GE, Luhr DR, Adaska WS. Guide to cement-treated base. Skokie (IL, USA): Portland Cement Association; 2006.
[87] Bravo M, de Brito J, Pontes J, Evangelista L. Mechanical performance of concrete made with aggregates from construction and demolition waste recycling plants. J Clean Prod 2015;99:59–74. https://doi.org/10.1016/j.jclepro.2015.03.012.
[88] Yan S, Wang B, Ma J, Lyu B. The effect of waste clay brick content on performance of cement-stabilized recycled concrete aggregate in pavement base and subbase applications. J Mater Civ Eng 2023;35:04023135. https://doi.org/10.1061/JMCEE7.MTENG-14807.
[89] Kongkitkul W, Saisawang T, Thitithavoranan P, Kaewluan P, Posribink T. Correlations between the surface stiffness evaluated by light-weight deflectometer and degree of compaction 2014:65–75. https://doi.org/10.1061/9780784413449.007.
[90] Louw S, Jones D. Pavement recycling: literature review on shrinkage crack mitigation in cement-stabilized pavement layers. Davis (CA, USA): California Department of Transportation Division of Research, Innovation and System Information; 2015 [accessed April 2, 2024], https://escholarship.org/uc/item/6qb3d9dx.
[91] Zhao X, Dong Q, Yuan J, Chen X, Yang J. Micro-scale characterization of the heterogeneous properties of in-service cement-treated base material. Constr Build Mater 2020;264:120696. https://doi.org/10.1016/j.conbuildmat.2020.120696.
[92] Bakare MD, Shahu JT, Patel S. Stress-dependent behavior of lightly stabilized industrial waste subbase using falling weight deflectometer. Geotech Test J 2024;47:371–91. https://doi.org/10.1520/GTJ20220283.
[93] Hossain S, Apeagyei A. Evaluation of the lightweight deflectometer for in-situ determination of pavement layer moduli. Richmond (VA, USA): Virginia Department of Transportation; 2010 [accessed January 5, 2017], http://ntl.bts.gov/lib/37000/37700/37795/10-r6.pdf.
[94] Apeagyei AK, Hossain M. Stiffness-based evaluation of base and subgrade quality using three portable devices. In: Proceedings of the 88th Transportation Research Board Annual Meeting; 2010.
[95] Lunkes Strieder H, Grassioli Schreinert G, Ferreira Matuella M, Fedrigo W, Delongui L, Rutzen D, et al. Mechanical behavior of construction and demolition waste as pavement materials: influence of mix composition and compaction conditions. Constr Build Mater 2023;408:133698. https://doi.org/10.1016/j.conbuildmat.2023.133698.
[96] Contreras M, Teixeira SR, Lucas MC, Lima LCN, Cardoso DSL, da Silva GAC, et al. Recycling of construction and demolition waste for producing new construction material (Brazil case-study). Constr Build Mater 2016;123:594–600. https://doi.org/10.1016/j.conbuildmat.2016.07.044.
[97] Moschen-Schimek J, Kasper T, Huber-Humer M. Critical review of the recovery rates of construction and demolition waste in the European Union – an analysis of influencing factors in selected EU countries. Waste Manag 2023;167:150–64. https://doi.org/10.1016/j.wasman.2023.05.020.
[98] Bonifazi G, Grosso C, Palmieri R, Serranti S. Current trends and challenges in construction and demolition waste recycling. Curr Opin Green Sustainable Chem 2025;53:101032. https://doi.org/10.1016/j.cogsc.2025.101032.
[99] European Committee for Standardization. Tests for geometrical properties of aggregates – Part 4: Determination of particle shape – shape index; 2008.
[100] European Committee for Standardization. Tests for geometrical properties of aggregates – Part 3: Determination of particle shape – flakiness index; 2012.
[101] European Committee for Standardization. Tests for mechanical and physical properties of aggregates – Part 6: Determination of particle density and water absorption; 2013.
[102] European Committee for Standardization. Tests for geometrical properties of aggregates. Part 11: Classification test for the constituents of coarse recycled aggregate; 2009.